Forcing mechanisms of intraseasonal SST variability off central Peru in 2000-2008

Serena ILLIG,
B. Dewitte, K. Goubanova, G. Cambon,
J. Boucharel, F. Monetti, C. Romero, S. Purca and R. Flores

1. Introduction

The Sea Surface Temperature (SST) **intraseasonal** variability ([40-90] *days*) along the coasts of Peru (**Fig1**) is commonly attributed to the efficient oceanic connection with the equatorial variability.

➤ In agreement with *Dewitte et al (2011)*, the **subseasonal SST** variability off Peru (**Fig1a**) consists in a narrow coastal fringe of SSTA with amplitudes decreasing from the coast to the offshore ocean. It highlight two regimes of variability (**Fig1b**) :

⇨ A wind forced sub-monthly regime (<40 day^{-1}) that explains 50%

⇨ An **intraseasonal regime** (40-90 day^{-1})

➤ Here, we focus on the **intraseasonal SST regime** (= 40% of subseasonal var). It shows a significant peak at ~60 days with a marked seasonal dependence, prominent in Austral Summer (**Fig1c**)

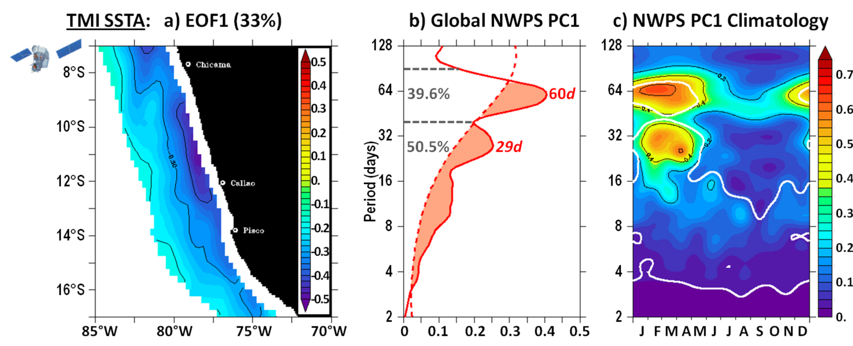

Fig1: Dominant mode of the **E**mpirical **O**rthogonal **F**unction analysis (EOF1) of the observed satellite TMI daily subseasonal SST anomalies (SSTA) that captures 33% of the variance. (a) Spatial pattern (°C). (b) Global Normalized Wavelet Power Spectrum (NWPS) of non-dimensional PC1-SSTA. Dashed line indicates the 95% confidence level and shading underlines significant global NWPS. (c) 8-year climatology of the NWPS estimated over June 2000 to May 2008. White line shows the 95% confidence level.

2. Objectives

What are **the forcing mechanisms** of the **intraseasonal SST variability** off central Peru (8°S-16°S) during the 2000-2008 period ?

Locally forced
Wind stress, Heat Fluxes ?

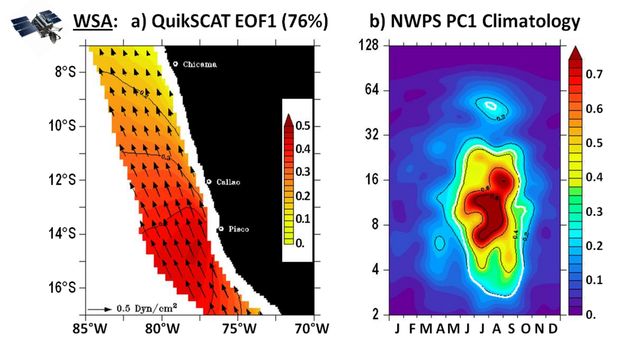

Fig2: First mode of the bivariate EOF analysis of the subseasonal anomalies of the surface wind stress components from QuikSCAT data: (a) Spatial pattern (dyn/cm²). (b) 8-year climatology of the NWPS for the wind stress PC1 (PC1-WSA) estimated over June 2000 to May 2008. White line shows the 95% confidence level.

➤ **Local wind stress** forcing shows upwelling favorable patter that is prominent in Austral Winter and barely significant at intraseasonal timescales **Fig2**

➤ Analysis of **Intraseasonal Equatorial Kelvin Wave** (IEKW) activity at 100°W shows that the remote equatorial forcing shares the temporal characteristics of the intraseasonal SST variability off Peru **Fig3**

Remote forcing
Connection with the equator

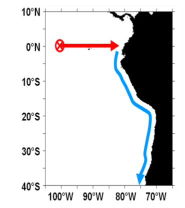

Fig3: Intraseasonal Equatorial Kelvin Wave (IEKW, estimated from SODA reanalysis) Sea Level contribution: Climatology of the NWPS for (c) the first and (d) the second baroclinic mode IEKW sea level contribution at 100°W. White line shows the 95% confidence level.

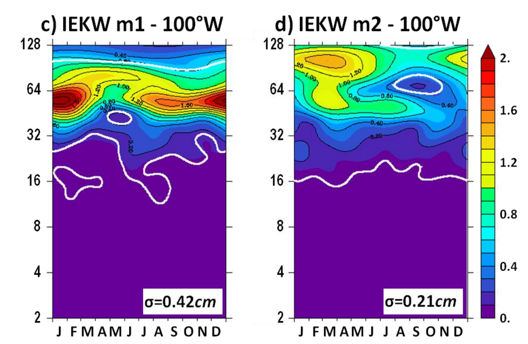

3. Methodology

Our approach is based on the experimentation with the regional ocean model ROMS

Model Configuration :

- Domain: [40°S-15°N ; 100°W-70°W]
- Horizontal resolution : 1/6°
- 32 (sigma) vertical levels
- Bathy GEBCO_08

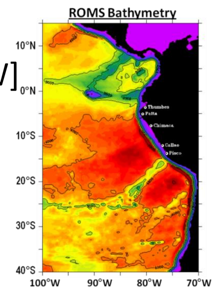

Model Forcing :

- Wind stress : QuikSCAT daily (CERSAT)
- Heat/Water Fluxes : Bulk formula with daily ERA-I
- Boundary Condition : SODA (5 days)
- Spin-up : 3 years (2000)
- Simulation over 2000-2008 with daily outputs

Model Validation :

Our confidence in the model configuration results in its realism as evidenced by the detailed validation of the model control run experiment ($ROMS^{CR}$) which indicates that it is **skillful** in simulating most aspects of the **mean state** and the **intraseasonal variability**.

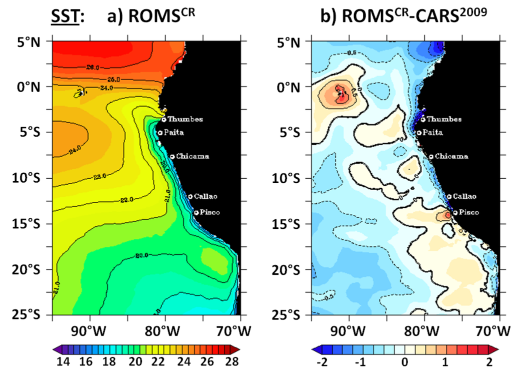

Fig4: (a) Map of the mean (2000-200) SST for $ROMS^{CR}$. (b) Differences between model and $CARS^{2009}$ data in °C.

- **Fig4**: The model has a good mean SST, with averaged bias < 0.5°C.
- Compared to **Fig1**, **Fig5** shows that the model captures the main characteristics of the dominant mode of intraseasonal SST variability off central Peru, with correlation (RMSdiff) between model and observed PC1-SSTA (**Fig5d**) of 0.88 (0.25°C).
- **Fig6**: The agreement between model Sea Level and AVISO data is statistically significant along the equatorial wave guide and its coastal extension, highlighting the efficient oceanic connection with the equatorial variability at intraseasonal times scales.

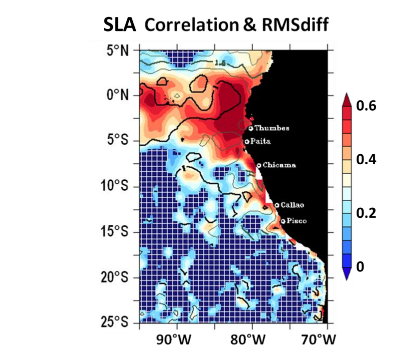

Fig6: Map of correlation (color) and RMSdiff (contours, in *cm*) between 7 day averaged intraseasonal sea level anomalies from $ROMS^{CR}$ and AVISO data. Blue square patterns mask non significant correlations (95% confidence level).

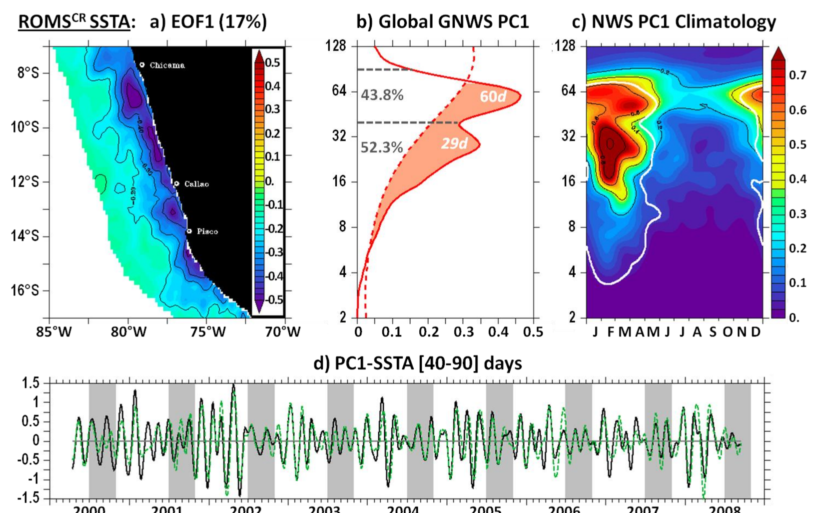

Fig5: Up: same as **Fig1** but for $ROMS^{CR}$ SST. Bottom: Intraseasonal band-pass filtered PC1-SSTA ([40-90] day^{-1}) for $ROMS^{CR}$ (black) and TMI (green). Grey bands show the July to October season.

Model Experimentation :

EXP-Name	OBC (E)	Wind Stress (W)	Heat Fluxes (Q)
$ROMS^{CR}$	Total	Total	Total
$ROMS^{E}$	Total	Climatology	Climatology
$ROMS^{WQ}$	Climatology	Total	Total
$ROMS^{W}$	Climatology	Total	Climatology

We carried out 4 experiments in order to assess the oceanic response to wind stress, heat fluxes and long equatorial waves at subseasonal timescales off central Peru and interpret the observations (**Fig1**). ⇨ Our experiments differ by their boundary conditions, either climatological or real-time (**Table 1**).

4. Remote equatorial forcing quantification

➡ Comparison of the model experiments reveals that the **intraseasonal SLA variability** off central Peru is accounted for by almost the sole equatorial forcing **Fig7**

The ratio of variance between $ROMS^{E}$ ($ROMS^{WQ}$) and $ROMS^{CR}$ estimated for the [40-90] day^{-1} scales for central Peru coastal SLA (averaged between 16°S-8°S within the 0.5° coastal fringe) is 95% (24%).

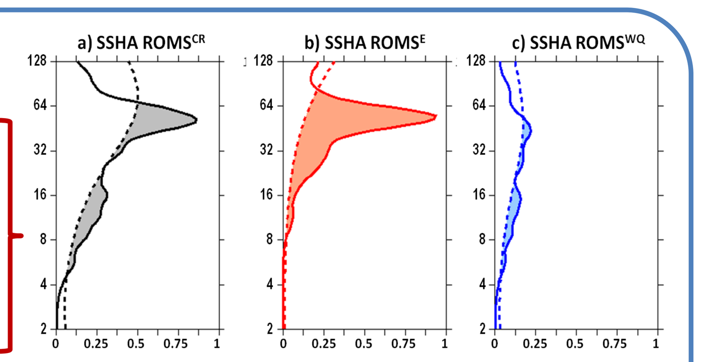

Fig7: Coastal (0.5° coastal band averaged) SSH averaged between 16°S and 8°S : (top) Global NWPS of subseasonal SSH for (a) $ROMS^{CR}$ simulation, (b) $ROMS^{E}$ simulation and (c) $ROMS^{WQ}$ simulation. Unit is cm². Dashed lines indicates the 95% confidence level.

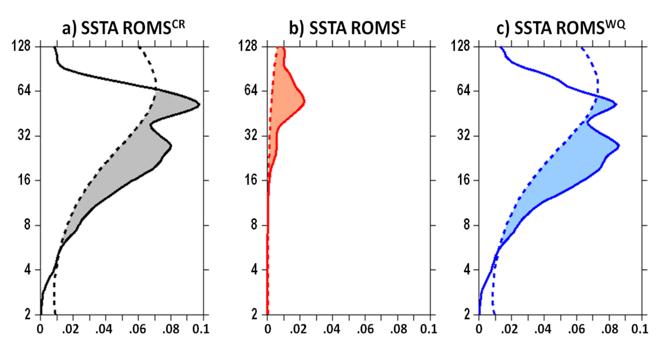

Fig8: Same as **Fig7** but for central Peru coastal SST analysis. Unit is °C².

➡ Connection with the remote equatorial variability is only marginally influential on the **intraseasonal SSTA variability**, as it represents only ~23% of the intraseasonal SST variability off Central Peru in 2000-2008 (**Fig8**) !

Conversely, the local forcing explains most of the intraseasonal SST variability along the coast of central Peru, since the spectrum for $ROMS^{CR}$ and $ROMS^{WQ}$ are comparable (ratio=93%) for the [40-90] day^{-1} scales.

Since the seasonal dependence of the intraseasonal wind stress activity (**Fig1c**) is different from the one of the SST (**Fig2b**), the model results are counter-intuitive. This calls for investigating the mixed-layer processes associated with the local atmospheric forcing.

5. Local forcing and processes

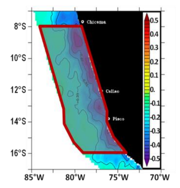

Fig9: Time-lagged composites of the intraseasonal anomalies of $ROMS^{WQ}$ simulation averaged between 16°S-8°S as a function of the distance from the coast (in 10^2 *km*) for intraseasonal cold events: temperature in the mixed layer (T_{MLD} in °C), along shore wind stress (100xdyn/cm²), surface net heat fluxes (Qnet in W/m²) and mixed layer depth (*h* in m).

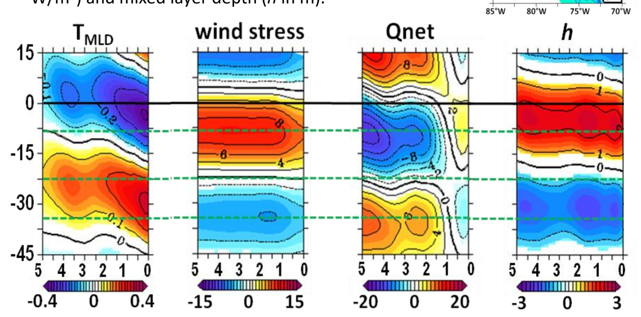

To filter out the internal model variability and provide an overview of the time sequence of intraseasonal cold events:

- We used a composite analysis of strongest intraseasonal SST events.
- Of latitudinal averages (16°S-8°S)
- Results are displayed as a function of the distance to the coast (**Fig9-10**).

- Black horizontal lines (—) ⇔ Mature phase of the event (@lag=0*day*), when the rate of change of T_{MLD} is zero.
- Green dashed lines (----) ⇔ characteristic of the wind stress activity
  - lag=-8*day* ↔ Max. of the upwelling favorable wind (>0.8 *dyn.cm*^-2^)
  - lag=-22*day* ↔ Min in alongshore wind stress @ lag=-22*day*)
  - lag=-33*day* ↔ Max of downwelling favorable wind stress

$$\partial_t\langle T\rangle = \underbrace{-\langle u\partial_x T\rangle}_{\text{X-ADV}} \underbrace{-\langle v\partial_y T\rangle}_{\text{Y-ADV}} \underbrace{-\langle w\partial_z T\rangle}_{\text{Z-ADV}} \underbrace{-\frac{1}{h}(k_z\partial_z T)_{z=-h}}_{\text{DIFF}} \underbrace{-\frac{1}{h}\partial_t h\times(\langle T\rangle - T_{z=-h})}_{\text{ENTR}} + \underbrace{\frac{Q^{*}+Q_S-Q_P}{\rho C_p h}}_{\text{FORC}}$$

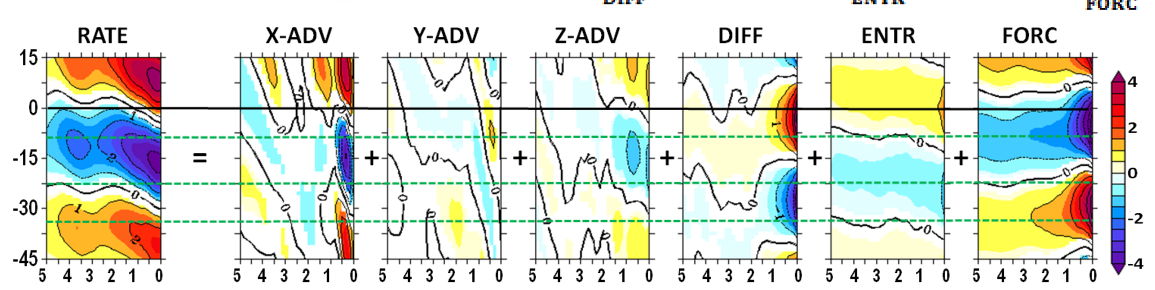

Fig10: Same as Fig9, for the $ROMS^{WQ}$ online intraseasonal heat budget within the mixed layer : rate of change, zonal, meridional and vertical advection terms, diffusivity at the base of the mixed layer, entrainment and forcing term. Unit is 100x°C/day. Color shading indicates significant composites (90% confidence level).

The analysis of the mixed-layer processes (**Fig10**) highlights the active role of the advection processes associated with **Ekman dynamics**. Still, due to the shallow mixed-layer during this season, **diabatic processes** have a significant contribution (~30%) which is influential on the evolution of SST anomalies. In particular, they favor a faster response of SST to wind stress, reducing the quadrature between SST and wind stress anomalies expected from a conceptual advective model ($\frac{dT}{dt} = -\tilde{w}.\frac{\partial \overline{T}}{\partial z}$).

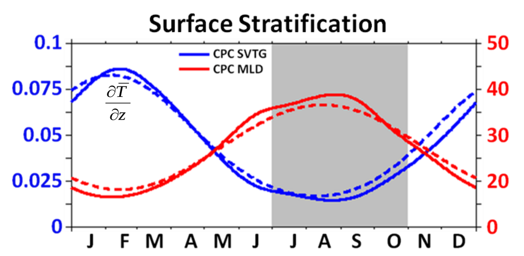

Fig11: Coastal (0.5° coastal band averaged) Surface Vertical Thermal Gradient (SVTG: difference between SST and temperature at 50*m* depth, blue, left scale, °C/meter) and Mixed Layer Depth (MLD, red, right scale, meters) averaged between 16°S-8°S for $ROMS^{CR}$ (plain lines) and $CARS^{2009}$ (dashed lines). Grey shading is the July to October season.

In austral winter, despite the strong wind stress variability (**Fig2**), the vertical advection is reduced:

⇨ **Surface stratification** characteristics = magnitude of the Surface Vertical Temperature Gradient (SVTG, **Fig11**) determines the efficiency by which wind stress anomalies force SST anomalies through advection processes (*Goubanova et al. (2013)*).

6. Summary and conclusions

Despite evidences of **clear propagations** of coastal trapped waves of equatorial origin observed in the thermocline fluctuations until 30°S (**Fig12**) and the comparable marked seasonal cycle in the intraseasonal Kelvin wave and coastal SST variability (*i.e.* peak in Austral summer) off central Peru, the **remote equatorial forcing only accounts for ~20% of the intraseasonal SST regime**, which instead is mainly forced by the local winds and heat-fluxes.

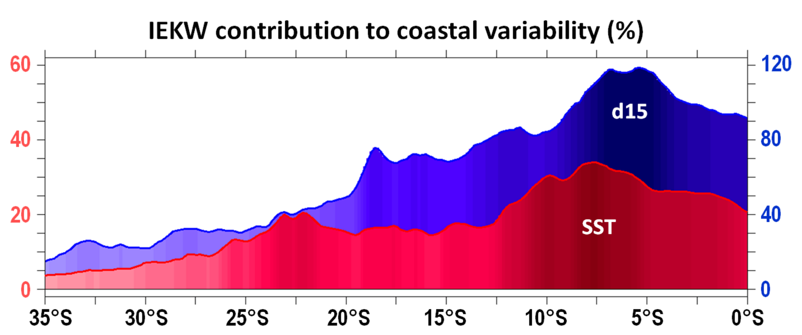

Fig12: Intraseasonal variability ratio (%) of variance between $ROMS^{E}$ simulation and $ROMS^{CR}$ as a function of latitude for the SST (red, left scale) and the depth of the 15°C isotherm (d15, blue, right scale) averaged in a 0.5° coastal band.

A heat budget analysis further reveals that during the Austral summer, despite the weak along-shore upwelling (downwelling) favourable wind stress anomalies, significant cool (warm) SST anomalies along the coast are to a large extent driven by **Ekman-induced advection**. This is shown to be due to the shallow mixed layer that increases the efficiency by which wind stress anomalies relates to SST through advection.

Thus, **the SST intraseasonal regime** during the Austral summer **is mostly wind-driven** despite the very weak wind stress variability (*i.e.* ~6 times weaker than in Austral winter).

Diabatic processes also contribute to the SST intraseasonal regime, which tends to shorten the lag between peak SST and wind stress anomalies compared to what is predicted from a simple advective mixed-layer model.

7. References and Acknowledgements

Dewitte, B., S. Illig, L. Renault, K. Goubanova, K. Takahashi, D. Gushchina, K. Mosquera, and S. Purca, 2011: Modes of covariability between sea surface temperature and wind stress intraseasonal anomalies along the coast of Peru from satellite observations (2000–2008), *J. Geophys. Res.*, **116**, C04028, doi:10.1029/2010JC006495.

Goubanova K., S. Illig, E. Machu, V. Garçon and B. Dewitte, 2013: SST subseasonal variability in the Benguela upwelling system as inferred from satellite observations (2000-2008), *J. Geophys. Res.-Oceans*, 2169-9291, doi: 10.1002/jgrc.20287.

This study has been published in JGR in June 2014 :
Illig S., B. Dewitte, K. Goubanova, G.Cambon, J. Boucharel, F. Monetti, C. Romero, S. Purca and R. Flores, 2014 : Forcing mechanisms of intraseasonal SST variability off central Peru in 2000-2008, *J. Geophys. Res.-Oceans*, 119, 3548-3573, doi:10.1002/2013JC009779.

web

We would like to thank the CNES (OSTST EBUS-SOUTH) and ESA (project OceanFlux) for financial support.
TMI data are produced by Remote Sensing Systems and sponsored by the NASA Earth Science MEaSUREs DISCOVER Project. Wind stress data were obtained from the Centre de Recherche et d'Exploitation Satellitaire (CERSAT), at IFREMER, Plouzané (France). We are grateful to Dr. B. Giese from Texas A&M University for providing the SODA outputs.
We are thankful to the DSI/IRD for supporting the SPIRALES project dedicated to the implementation of a cluster at IMARPE (P.I: B. Dewitte) over which the model configuration used in this study was developed and most simulations were performed. Some were also performed on the CALMIP computer at University Paul Sabatier (Toulouse, France, CALMIP project 1044). The model grid, forcing, and initial conditions were built using the ROMSTOOLS package (Penven et al., 2008). The authors wish to acknowledge use of the Ferret program (NOAA PMEL, http://ferret.pmel.noaa.gov) for analysis and graphics.